

Strength Characteristics of Calcareous Sands with Different Particle Size Based on Triaxial Tests

Y. Gao¹, W. L. Li^{1*}, H. Y. Zhang¹ and H. Chen¹

¹Associate professor, Guangdong Provincial Key Lab of Geodynamics and Geohazards, School of Earth Sciences and Engineering, Sun Yat-sen University, Guangzhou, Guangdong 510275, China. gaoyan25@mail.sysu.edu.cn

^{1*} Corresponding author. Graduate student, Guangdong Provincial Key Lab of Geodynamics and Geohazards, School of Earth Sciences and Engineering, Sun Yat-sen University, Guangzhou, Guangdong 510275, China. liwl26@mail2.sysu.edu.cn

Abstract: Calcareous sand with the characteristics of high internal porosity, irregular shape and fragileness, should have particular strength properties compared with silica sand. In order to explore its strength characteristics, calcareous sands from an island in the South China Sea were divided into 4 groups according to the particle size: < 0.5 mm, 0.5 ~ 1 mm, 1 ~ 2 mm, and 2 ~ 5 mm, and then triaxial compression tests were conducted, respectively. The test results show that the stress-strain curve of calcareous sands can be classified into two types according to whether the particle breakage controls or not. The parameters of relative particle breakage B_r and the related broken limit confining pressure P_b were used. When $B_r < 0.1$, $\sigma_3 < P_b$, the particle breakage of the sample can be neglected, and the sample behaves dilatation and strain softening. When $B_r > 0.1$, $\sigma_3 > P_b$, the behavior of the sample is dominant by the particle breakage, which shows contraction and strain hardening. Under low confining pressure, the peak value of σ_1/σ_3 for the large-size sample is much higher than that for the small-size sample; with the increase of σ_3 , the peak value of σ_1/σ_3 for the large-size sample decreases gradually and even smaller than that for small-size samples due to the increase of particle breakage; the internal friction angles of calcareous sands are mainly concentrated at $33^\circ \sim 35^\circ$ under low confining pressure; with the increase of particle size, the inter locking between irregularly shaped particles increases, the cohesion increases, $\varphi_p - \varphi_{cs}$ decreases, and the dilatancy of the samples decreases. Under middle-high confining pressure, the internal friction angles are mainly concentrated at $23^\circ \sim 35^\circ$; with the increase of particle size, $\varphi_p - \varphi_{cs}$ gradually decreases, and the sample behavior changes from dilatation to contraction. From the initial stage of the test to the phase-change point, the deformation of the sample is mainly caused by the pore compaction between particles and the dilatation caused by the particles climbing slope. With the increase of particle size, the compression coefficient C_c of the sample gradually increases, while the dilatation coefficient C_d and the dilatation-contraction ratio S_d gradually decreases. From phase-change point to the critical state, the deformation of the sample is mainly caused by the breakage and rearrange of particles, the characteristic value of dilatation curve $\tan\psi_{max}$ decreases with the increase of particle size.

Keywords: calcareous sands, particle size, particle breakage, triaxial compression test, dilatancy.

1. Introduction

Calcareous sands are the marine-biogenic granular material with the content of calcium carbonate larger than 50%, which are mostly distributed near the islands and reefs between 30° north latitude and 30° south latitude, such as the islands of the South China Sea, Arabian Gulf, the Red Sea, western continental shelf of Australia and other places (Liu et al. 1998, 1999). With the development of marine resources, calcareous sands become a very important material for island projects. Hence, the research on strength characteristics of calcareous sands is of great significance for the rapid development of island projects.

At the beginning of the twentieth century, scholars have already found the particle breakage of silica sands under high pressure (DeBeer et al. 1963). In the 1960s and 1970s, the engineering accidents of calcareous sands foundation made people realize the importance of particle breakage for calcareous sands. Therefore, many scholars have carried out a lot of studies on calcareous sands particle breakage. Coop et al. (1990, 1993) and Georgoutsos et al. (2004) made a comprehensive study on the strength of calcareous sands, and the test results showed that the drained shear strength of calcareous sands was similar to that of clay, and with the increase of effective confining pressure, the strain required to achieve the final stress ratio became larger. Fahey (1988) found that the shear properties of calcareous sands were different under low and high confining pressures. Fookes

(1988) classified calcareous sands according to particle size, mineral composition and strength characteristics from the perspective of engineering application.

In 1998, the international conference on calcareous sediments was held in Australia, which summarized the origin, engineering characteristics and the future development of calcareous sands, which greatly promoted the scientific research of calcareous sands. At present, the strength of calcareous sands is mainly studied by laboratory test. And many scholars have conducted a large number of triaxial tests to explore the effects of confining pressure, particle size, strain and other factors on the particle breakage and strength of calcareous sand (Sun and Wang et al. 2003, 2004, 2006, Zhang et al. 2008, 2009, Jiang et al 2015, Alaa et al. 2018, Weng et al. 2019). Hu (2008) explored the factors that can affect calcareous sand particle breakage through a large number of triaxial tests and modified the constitutive model of calcareous sands. Ma (2016) found that the cohesive force of calcareous sands was positively correlated with particle size through large-scale direct shear tests. Giang et al. (2017) studied the effect of particle size distribution on small strain shear modulus. Chen et al. (2018) analyzed the relationship between the relative density and particle breakage of calcareous sands through the triaxial tests, and explained the influence of particle movement and breakage on the strength from a microscopic perspective. Chen (2019) conducted a study on the particle

morphology and mechanical characteristics of calcareous silt, and found the contribution of particle morphology to the inter locking and the influence of relative density on the strength of calcareous sand. In addition, some scholars have also carried out a comparative study on the properties of siliceous sands and calcareous sands. Suescan-florez et al. (2017), Ma and Liu et al. (2018) summarized the particle breakage and strength characteristics of silica and calcareous sands under high stress with different strain rates through laboratory tests. In order to improve the strength of calcareous sands, in recent years, some scholars have carried out experimental studies on microbial cemented calcareous sands, and achieved a good strength improvement (Zhu et al. 2014a, 2014b, 2015, Liu et al. 2018).

The previous studies show that the particle shape and particle size has a good correlation (Yuan et al. 2019), also related to the strength. At present, the research on the strength of calcareous sand is mostly focused on a certain particle size range, and the influence of particle size on its strength and the change of dilatancy is less. Therefore, in this paper, calcareous sands were divided into four groups according to particle size: < 0.5 mm, 0.5 ~ 1 mm, 1 ~ 2 mm, 2 ~ 5 mm, and triaxial compression tests were carried out on these 4 groups of samples to explore the effects of particle size on the strength and dilatancy of calcareous sands.

2. Experimental details

In this paper, an automatic stress path triaxial instrument was used to do triaxial compression tests on 4 groups of calcareous sands samples with different particle size, i.e., < 0.5 mm, 0.5 ~ 1 mm, 1 ~ 2 mm and 2 ~ 5 mm, respectively. The initial relative density of the samples was 70%, which was in a dense state. After the samples were saturated with B value larger than 0.98, drained triaxial compression tests were begun. Hence, the total stress and the effective stress were the same in this paper. In order to ensure the comparability of each test and avoid particle breakage during sample preparation, the sands were put into the mold in five times, and compacted layer by layer with wooden blocks to the required density.

The triaxial test was carried out according to the standard “GB-T50123-2019”. The effective confining pressure σ_3 of each group were 50 kPa, 100 kPa, 200 kPa, 400 kPa, 600kPa, and 800 kPa, respectively. The compression rate was 0.3 %/min, and the test was stopped when the axial strain reached 20%. During the test, the pore water pressure was always 0. The axial strain ε_a , the volumetric strain ε_v , the axial stress σ_1 and the effective confining pressure σ_3 were recorded. The degree of particle breakage of calcareous sands was quantitatively characterized by the relative particle breakage B_r (Hardin 1985).

3. Experimental Results and Analysis

3.1 stress-strain curve

Fig. 1 and Fig. 2 show the typical diagrams of strain softening and strain hardening in triaxial compression tests, respectively. During the testing process, the strain localization and shear band were observed for the sample

with strain softening (Figure 1); while the shear band cannot be formed in the sample with strain hardening (Figure 2) due to the breakage and rearrangement of soil particles.

Figs. 3 ~ 6 illustrate the stress-strain relationships of 4 groups of dense calcareous sand samples. A similar behavior was obtained. That is, with the increase of confining pressure σ_3 , the peak value of σ_1/σ_3 gradually decreased, while the volumetric strain ε_v of sample changed from dilation to contraction. ε_v was the result of the combined action of pore compaction and particle breakage. With the increase of σ_3 , a larger B_r was obtained which indicated an increasing particle breakage (Fig. 7), which in turn led to the contraction of the sample. It is also found that B_r for samples with different particle sizes has a good logarithmic relationship with the confining pressures. Since the samples with different particle sizes have different particle breakage, the confining pressure corresponding to the volume change from dilatation to contraction is different. In this paper, the broken limit confining pressure for the particle breakage was adopted, labeled as P_b , and the relative particle breakage $B_r = 0.1$ was taken as the boundary (Fig. 7). When $B_r < 0.1$, $\sigma_3 < P_b$, the particle breakage of the sample could be neglected, and the sample dilatation. When $B_r > 0.1$, $\sigma_3 > P_b$, the particle breakage of the sample was dominant, and the sample tended to contraction. P_b for the samples with different particle size of 0.5 ~ 1 mm, 1 ~ 2 mm and 2 ~ 5 mm was 600 kPa, 400 kPa and 200 kPa, respectively. Under the conventional pressure, particle breakage of samples with particle size less than 0.5 mm can be neglected, and there was no broken limit confining pressure P_b .

Particle shape is various for different particle sizes. With the increase of particle size, the shape of calcareous sands becomes more irregular, and the inter locking between the particles increases (Yuan et al. 2019). Under low confining pressure (Fig. 3 ~ Fig. 6), large-size samples had a higher inter locking, which made the peak value of σ_1/σ_3 much higher than that of small-size samples. With the increase of σ_3 , on account of the increasing breakage and the decreasing inter locking of the particles, the peak value of σ_1/σ_3 with large-size sample was gradually reduced and even smaller than that of small-size samples. It is speculated that when $\sigma_3 > 400\text{kPa}$, calcareous sand particles produced obviously breakage, mainly due to the grinding of the edges and corners of the particles. Hence, the increasing small-size particles in the shear zone enhanced the lubrication for deformation and reduced the strength.

When the samples entered a critical state, σ_1/σ_3 values for samples with particle size less than 1mm finally became consistent. The σ_1/σ_3 values for samples with particle size larger than 1mm under low confining pressure was greater than that under high confining pressure, especially when the particle size was larger than 2 mm, and the possible reason is that particle breakage is more severe in the samples with high confining pressure and large particle size (Fig. 7) and the interparticle locking decreases, which leads to a decrease in the value of σ_1/σ_3 .

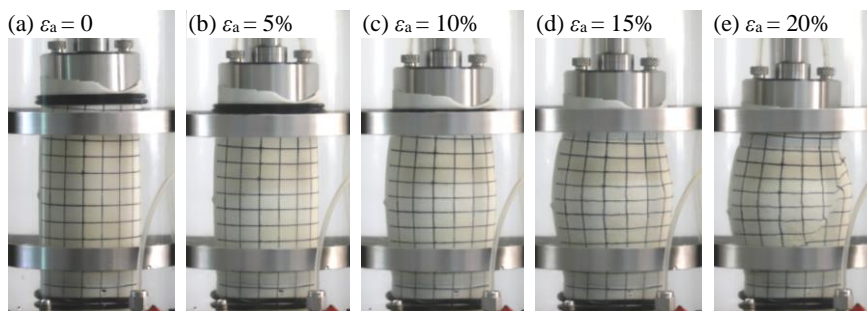


Figure 1. Triaxial drained compression test results for particle diameter $< 0.5\text{ mm}$ under 600 kPa confining pressure ($\sigma_3 = 600\text{ kPa}$): (a) $\epsilon_a = 0\%$; (b) $\epsilon_a = 5\%$; (c) $\epsilon_a = 10\%$; (d) $\epsilon_a = 15\%$; and (e) $\epsilon_a = 20\%$.

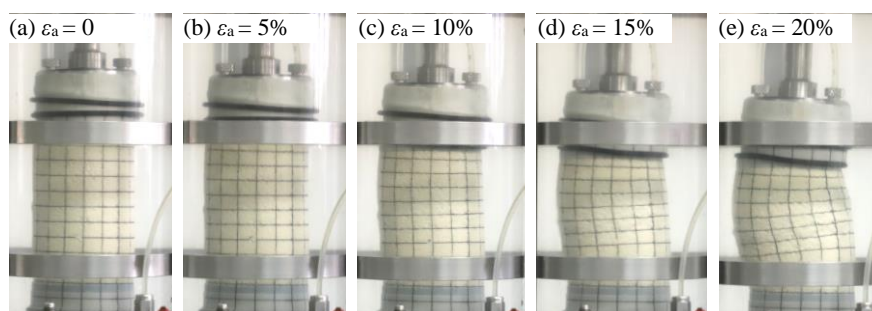


Figure 2. Triaxial drained compression test results for particle diameter $0.5 \sim 1\text{ mm}$ under 600 kPa confining pressure ($\sigma_3 = 600\text{ kPa}$): (a) $\epsilon_a = 0\%$; (b) $\epsilon_a = 5\%$; (c) $\epsilon_a = 10\%$; (d) $\epsilon_a = 15\%$; and (e) $\epsilon_a = 20\%$.

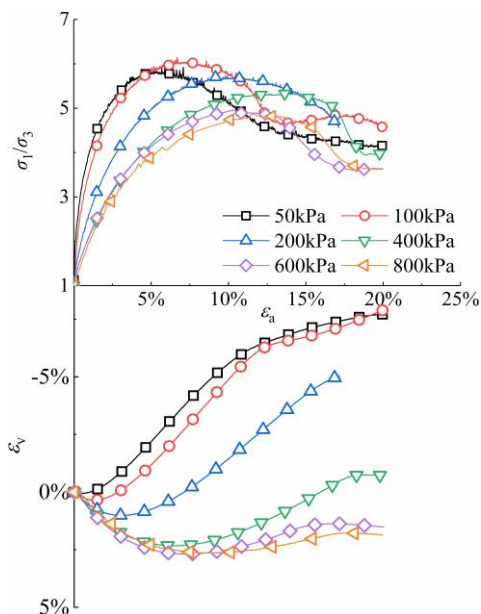


Figure 3. σ_1/σ_3 and $\epsilon_v \sim \epsilon_a$ (particle size $< 0.5\text{ mm}$).

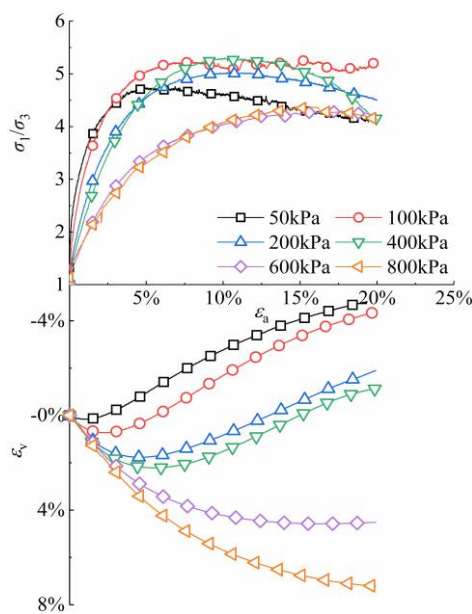


Figure 4. σ_1/σ_3 and $\epsilon_v \sim \epsilon_a$ (particle size $0.5 \sim 1\text{ mm}$).

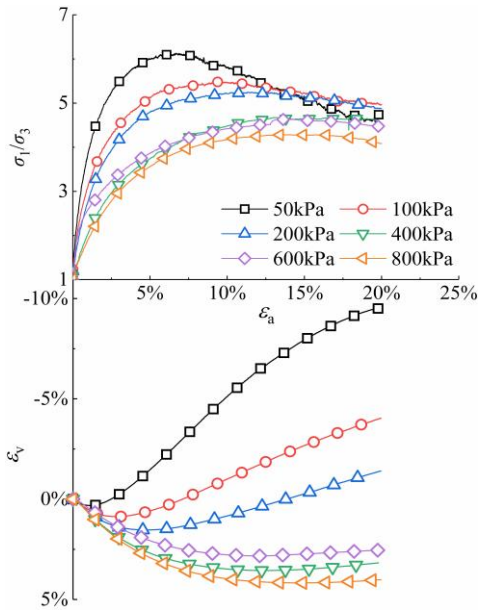


Figure 5. σ_1/σ_3 and $\varepsilon_v \sim \varepsilon_a$ (particle size 1 ~ 2 mm).

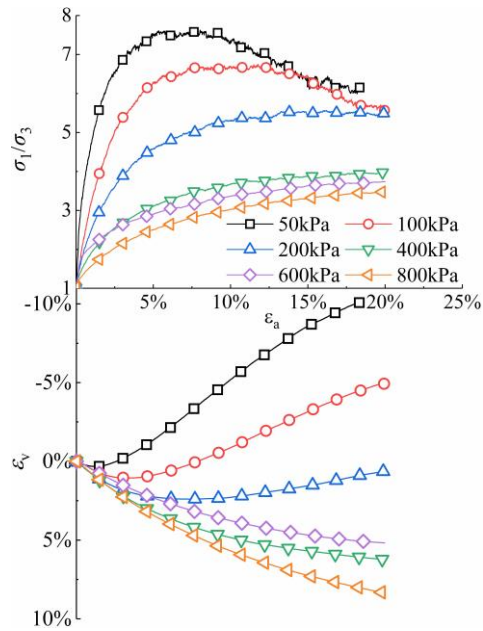


Figure 6. σ_1/σ_3 and $\varepsilon_v \sim \varepsilon_a$ (particle size 2 ~ 5 mm).

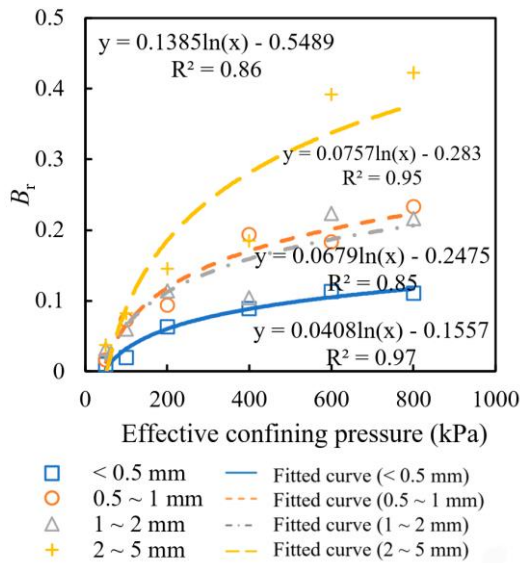


Figure 7. The relative particle breakage B_r .

3.2 Strength (c, φ)

Considering the different degrees of particle breakage of calcareous sands under low and middle-high confining pressure, the strength parameters (cohesion c and internal friction angle φ) of calcareous sands with particle diameter $> 0.5\text{mm}$ were classified into two groups: at low pressure and relatively middle-high pressure. Herein, the boundary is broken limit confining pressure P_b . The particle breakage of calcareous sands under low confining pressure can be neglected and its strength is mainly controlled by particle size and shape. Since calcareous sands have obvious particle breakage under middle-high confining pressure, its strength is greatly

affected by particle breakage. According to the standard “GB-T50123-2019” for geotechnical test methods, the maximum value of the axial stress or the axial stress at $\varepsilon_a = 5\%$ is taken as the peak strength, and the axial stress at $\varepsilon_a = 15\%$ is regarded as the residual strength. Table 1 and Table 2 summarize the value of c and φ for calcareous sands. c_p, φ_p are the peak strength while c_{cs}, φ_{cs} represents residual strength. Calcareous sands are different from the terrestrial siliceous sands. Calcareous sands, due to its irregular particle shape, have obvious interparticle locking, which is the main source of its cohesion (Wang et al., 2018). It can be seen from Table 1 that under low confining pressure, the internal friction angles of calcareous sands are mainly concentrated at $33^\circ \sim 35^\circ$. When the particle size increases, the more irregular the shape of the particles is, the greater the internal friction angle is. At the same time, the interparticle locking increases, which induces an increasing cohesion and decreasing dilatancy. A decreasing value of $\varphi_p - \varphi_{cs}$ is obtained. That is, the dilatancy decreases with the increase of particle size.

Under middle-high confining pressure, the increasing of confining pressure leads to the particle breakage increasing in the shear zone. The particles are broken from irregular branchlike and flake shapes into relatively regular spherical and spindle shapes, which further reduces the internal friction angles of calcareous sands to $23^\circ \sim 35^\circ$. Moreover, with the increase of particle size, $\varphi_p - \varphi_{cs}$ also decreases, which indicates that the dilatancy decreases. The interparticle locking increases with the increase of confining pressure. Therefore, compared with the low confining pressure, c_p and c_{cs} increase significantly with the confining pressure. With the increase of the particle size, $c_p - c_{cs}$ also increases gradually.

Table 1. Cohesion of calcareous sands with different particle sizes (unit: kPa).

Cohesion		Particle diameter			
		< 0.5 mm	0.5 ~ 1 mm	1 ~ 2 mm	2 ~ 5 mm
Under	c_p	25.44	1	5.5	18.66
lower	c_{cs}	9.53	1.68	1.59	14.6
pressure	$c_p - c_{cs}$	15.91	-0.68	3.91	4.06
Under	c_p	25.44	7.58	55.52	122.21
middle-high	c_{cs}	9.53	99.34	61.5	125.25
pressure	$c_p - c_{cs}$	15.91	-91.76	-5.98	-3.04

Table 2. Internal friction angles of calcareous sands with different particle sizes (unit: °).

Friction angle		Particle diameter			
		< 0.5 mm	0.5 ~ 1 mm	1 ~ 2 mm	2 ~ 5 mm
Under	ϕ_p	33.04	33.8	33.87	33.83
lower	ϕ_{cs}	32.53	33.4	33.83	33.89
pressure	$\phi_p - \phi_{cs}$	0.51	0.4	0.04	--
Under	ϕ_p	33.04	34.47	30.52	23.67
middle-high	ϕ_{cs}	32.53	29.86	30.82	25.08
pressure	$\phi_p - \phi_{cs}$	0.51	4.63	--	--

3.3 Dilatancy

The dilatancy of sandy soil is one of the important issues of soil mechanisms, which is an essential parameter for the constitutive model. From the initial stage to the phase-change point ($d\varepsilon_v/d\varepsilon_a = 0$) during the test, the contraction of the sand is mainly caused by pore compaction between particles and dilatation caused by particles “climbing slope”. From the phase-change point to the critical state, the deformation of samples is accompanied by obvious particle breakage and rearrangement. The deformation characteristics of calcareous sand are discussed in these two stages and different parameters are used.

The dilatation-contraction ratio S_d (Wei 1963) can express the compression and dilatation characteristics of the samples, and is suitable to describe the deformation characteristics of calcareous sand from the initial point to the phase-change point. However, when particle crushing significantly, the measure error becomes large. Hence, the characteristic value of dilatation curve $\tan\psi_{\max}$ is utilized to describe the deformation characteristics of calcareous sands from phase-change point to the critical state, which is more simply and intuitively.

3.3.1 Before phase-change point ~ dilatation-contraction ratio (S_d)

Skempton (1948) and Henkel (1960) proposed that the volume change of soil under external load can be calculated by the following equation,

$$\Delta V/V = C_c \Delta\sigma'_m + C_d \Delta\tau_m \quad (1)$$

$$S_d = C_d/C_c \quad (2)$$

where, C_c is the coefficient of volume compression; C_d is the coefficient of dilatation; the smaller C_d is, the greater the dilatancy is; $\Delta\sigma'_m$ is the increment of effective average compressive stress (octahedral compressive

stress); $\Delta\tau_m$ is the increment of deviatoric stress (octahedral shear stress); S_d is the modified structure coefficient (dilatation-contraction ratio), which can describe the dilatancy of sand under drained conditions. The negative value of S_d means dilatancy. The smaller S_d is, the greater dilatancy is.

For the triaxial test, $\Delta\sigma'_m = p = 1/3(\sigma'_1 + 2\sigma'_3)$, $\Delta\tau_m = q = \sigma'_1 - \sigma'_3$, therefore, C_c and C_d can be obtained through fittings by Eq. 1, then S_d can be obtained. In this paper, the phase-change points of samples in each group were selected to calculate S_d . The results are shown in Table 3 where R^2 is the goodness of the fitting. It is clear to see that the dilatancy and compressibility index of calcareous sand C_c and C_d are on the same order of magnitude. With the increase of the particle size, C_c increases gradually, that is, the sample compressibility increases; C_d decreases, which means the dilatation increases. The dilatation-contraction ratio S_d of the samples in all group are between -0.52 and 0.19, and S_d decreases with the particle size, that is, the dilatations of the samples gradually increase. The macroscopic compression deformation of the sample is the result of the interaction between the pores compaction and the dilatation caused by particle “climbing slope” and particle rearrangement.

Table 3. The fitting results of dilatation-contraction ratio S_d on different particle size group.

Particle size (mm)	C_c	C_d	S_d	R^2
< 0.5	8.57E-10	1.63E-10	0.19	0.86
0.5 ~ 1	5.59E-09	-2.16E-09	-0.39	0.89
1 ~ 2	7.52E-09	-3.13E-09	-0.42	0.99
2 ~ 5	1.39E-08	-6.32E-09	-0.46	0.98

3.3.2 After phase-change point ~ characteristic value of dilatation curve ($\tan\psi_{\max}$)

ψ_{\max} is the angle between the $\varepsilon_v \sim \varepsilon_a$ curve and the horizontal axis at the peak strength (Chang et al. 2010). The larger $\tan\psi_{\max}$ represents the more obvious dilatancy of the sample. The Table 4 shows calculated results of $\tan\psi_{\max}$. With the increase of the confining pressure, the degree of particle breakage increase, while $\tan\psi_{\max}$ reduces gradually until disappears. The sample deformation changes from dilatation to contraction. The confining pressure related to disappearance of $\tan\psi_{\max}$ is the same as P_b for each sample. Between the phase-change point to the critical state, sample deformation is mainly caused by particle breakage and rearrangement, therefore, the greater the particle size is, particle shape is more irregular and the particle is much easier to break. Hence, a decreasing $\tan\psi_{\max}$ is obtained. That is, dilatancy decreases with increasing particle size.

Table 4. Characteristic value of dilatation curve ($\tan\psi_{\max}$) of each sample under different confining pressure.

Particle size σ_3 (kPa)	< 0.5 mm	0.5~1 mm	1 ~ 2 mm	2 ~ 5 mm
50	1.23	0.67	1.04	0.82
100	1.16	0.58	0.47	0.41
200	0.85	0.39	0.31	--
400	0.58	0.44	--	--
600	0.20	--	--	--
800	0.16	--	--	--

4. Conclusions

The strength characteristics of calcareous sands can be seriously affected by the particle breakage. Four groups of calcareous sands samples with different particle size of < 0.5 mm, 0.5 ~ 1 mm, 1 ~ 2 mm and 2 ~ 5 mm were tested by the triaxial apparatus. The main conclusions are as follows.

(1) The relative particle breakage B_r and the related limit confining pressure P_b were used to characterized the particle breakage. When $B_r < 0.1$, $\sigma_3 < P_b$, the particle breakage of the sample can be neglected, and the sample shows dilatation and strain softening. When $B_r > 0.1$, $\sigma_3 > P_b$, the particle breakage of the sample is dominant, and the sample shows contraction and strain hardening;

(2) B_r of calcareous sands samples in each testing group has a good logarithmic relationship with the confining pressure, and the peak value of σ_1/σ_3 decreases with the increase of confining pressure. Under low confining pressure, the peak value of σ_1/σ_3 for large-size sample is much higher than that for small-size sample. With increasing σ_3 , the peak value of σ_1/σ_3 for the sample with large particle size reduce gradually and even smaller than that for the sample with small size particles;

(3) Under low confining pressure, the internal friction angles of calcareous sands are mainly concentrated at $33^\circ \sim 35^\circ$. As the particle shape becomes more irregular with

the increase of particle size, the cohesion is positively correlated with particle size. Under middle-high confining pressure, the particle breakage significantly reduces the internal friction angle which mainly concentrated at $23^\circ \sim 35^\circ$. $\varphi_p - \varphi_{cs}$ decreases gradually with the increase of particle size, and the sample deformation changes from dilatation to contraction.

(4) The deformation characteristics of calcareous sand can be divided into two stages. One is from the initial point to the phase-change point, in which the deformation of the sample is mainly caused by pore compaction between particles and the dilatation caused by particle "climbing slope". With the increase of particle size, the compressibility and dilatancy of the sample gradually increase while the dilatancy increases greatly. From the phase-change point to the critical state, the deformation of the sample is mainly dominated by particle breakage and rearrangement. With the increase of particle size, the volume of sample contracts significantly due to the effect of particle breakage.

Acknowledgement

The research was supported by National Natural Science Foundation of China (41807244) and Natural Science Foundation of Guangdong Province (2018A0303130154).

References

- Alaa, A., Salem, T. N. and Hassan, R. 2018. Geotechnical characterization of the calcareous sand in northern coast of Egypt. *Ain Shams Engineering Journal*, 9(4): 3381-3390.
- Henkel, D. J.1960. The shear strength of saturated remoulded clay. In *Proceedings of the ASCE Research Conference on Shear Strength of Cohesive Soils*. Boulder, CO, USA: [s. n.], 533–554.
- Chen, H. D., Wei, H. Z., Meng, Q. S., Wang, Z. B., and Feng, Z. 2018. The study on stress-strain-strength behavior of calcareous sand with particle breakage. *Journal of Engineering Geology*, 26(06), 1490-1498. (in Chinese)
- Chen, M. 2019. Research on physical and mechanical properties of calcareous silt and its weakening mechanism of calcareous sand strength. Guangxi University. (in Chinese)
- Chang, Z., Yang, J. and Cheng, X. H. 2010. Granular mechanical analysis of the strength and dilatancy of sands. *Engineering Mechanics*, 27(4), 95-104. (in Chinese)
- Coop, M. R. 1990. The mechanics of uncemented carbonate sands. *Géotechnique*, 40(4), 607-626.
- Coop, M. R., and Atkinson, J. H. 1993. The mechanics of cemented carbonate sands. *Géotechnique*, 43(1), 53-67.
- Debeer, E. E. 1963. The scale effect in the transposition of the results of deep sounding tests on the ultimate bearing capacity of piles and caisson foundations. *Géotechnique*, 13(1), 39-75.
- Fookes, P. G. 1988. The geology of carbonate soils and

- rocks and their engineering characterisation and description. *Engineering for calcareous sediments*, Rotterdam, Balkema. 2: 787-806.
- Fahey, M. 1988. The response of calcareous soil in static and cyclic triaxial test engineering for calcareous sediments." Proc., In *Proceedings of the International Conference on calcareous Sediments*. Perth, Australia, 1988. (2), 61-68.
- Giang, P. H. H., Van, I. P. O., Van, I. W. F., Menge, P. and Haegemana, W. 2017. Small-strain shear modulus of calcareous sand and its dependence on particle characteristics and gradation. *Soil Dynamics and Earthquake Engineering*, 100: 371-379.
- Georgoutsos, G., Bodas F. T., Sorensen, K. K., and Coop, M. R. 2004. Particle breakage during shearing of a carbonate sand. *Géotechnique*, 54(3), 157-163.
- Hardin, B. O. 1985. Crushing of Soil Particles. *Journal of Geotechnical Engineering*, 111(10), 1177-1192.
- Hu, B. 2008. Research on the particle breakage mechanical characteristic and constitutive model of calcareous sand under triaxial conditions. Wuhan: Institute of Rock and Soil Mechanics, Chinese Academy of Sciences. (in Chinese)
- Liu, H. L., Xiao, P., Xiao, Y., Wang, J. P., Chen, Y. M. and Chu, J. 2018. Dynamic behaviors of MICP-treated calcareous sand in cyclic tests. *Chinese Journal of Geotechnical Engineering*, 2018, 40(1): 38-45. (in Chinese)
- Lu, J., Fan, J. H., Wang, Z. J. and Huo, Z. S. 2015. Mechanical property of calcareous sand under action of compaction. *Global Geology*, 18(3), 183-187.
- Liu, C. Q., Yang, Z. Q., and Wang, R. 1995. Research status and progress of mechanical properties of calcareous soil. *Rock and Soil Mechanics*, (4), 74-84. (in Chinese)
- Liu, C. Q. and Wang, R. 1998. Physical and mechanical properties of calcareous sand. *Rock and Soil Mechanics*, 19(1), 32-38. (in Chinese)
- Ma, L. 2016. Experimental study of shear characteristics of calcareous gravelly soil. *Rock and Soil Mechanics*, 37(S1):309-316. (in Chinese)
- Ma, Q. F., Liu, H. L., Xiao, Y. and Jiang, X. 2018. Compression and particle breakage features of calcareous sand under high stress. *Journal of Disaster Prevention and Mitigation Engineering*, 38(6): 1020-1025. (in Chinese)
- Skempton, A. W. 1948. A study of the immediate triaxial test on cohesive soils. In *Proceedings of the 2nd Int. Conf. Soil Mech.*, Rotterdam, 1948. 1, 192-196.
- Suescun-Florez, E. and Iskander, M. 2017. Effect of fast constant loading rates on the global behavior of sand in triaxial compression. *Geotechnical Testing Journal*, 40(1): 52-71.
- Sun, J. Z., and Wang, R. 2003. Study on particle failure process of calcareous sand under triaxial compression. *Rock and Soil Mechanics*, (5), 822-825. (in Chinese)
- Sun, J. Z., and Wang, R. 2004. Influence of confining pressure on particle breakage and shear expansion of calcareous sand. *Chinese Journal of Rock Mechanics and Engineering*, 23(4), 641-644. (in Chinese)
- Sun, J. Z., and Luo, X. W. 2006. Study on a two-yield surface model with consideration of state-dependent dilatancy for calcareous sand. *Chinese Journal of Rock Mechanics and Engineering*, 25(10), 2145-2149. (in Chinese)
- Wang, X. Z., Weng, Y. L., Wang, X. and Chen, W. J. 2018. Interlocking mechanism of calcareous soil. *Rock and Soil Mechanics*, 39(09), 3113-3120. (in Chinese)
- Weng, Y. L., Yin, J., Chen, W. J., Yu, K. F., and Wang, X. Z. 2019. Influencing Factors for Particle Breakage of the Calcareous Sand under Triaxial Tests. *Soil Engineering and Foundation*, 33(03), 295-298. (in Chinese)
- Wei, R. L. 1963. Discussion on the dilatancy of soil. *Journal of Hydraulic Engineering*, (06):31-40. DOI: 10.13243/j.cnki.slx.1963.06.003. (in Chinese)
- Yuan, Q., Li, W. L., Gao, Y., Zhang, H. Y. and Wu, Z. Y. 2020. Experimental study on particle characteristics of calcareous sand and effect on its compressibility. *Journal of Hydroelectric Engineering*, 39(02):32-43. (in Chinese)
- Zhang, J. M., Jiang, G. S., and Wang, R. 2009. Research on influences of particle breakage and dilatancy on shear strength of calcareous sands. *Rock and Soil Mechanics*, 30(07), 2043-2048. (in Chinese)
- Zhang, J. M., Zhang, L., Jiang, G. S., and Wang, R. 2008. Research on particle crushing of calcareous sands under triaxial shear. *Rock and Soil Mechanics*, (10), 2789-2793. (in Chinese)
- Zhu, C. Q., Zhou, B. and Liu, H. F. 2014a. Investigation on strength and microstructure of naturally cemented calcareous soil. *Rock and Soil Mechanics*, 35(6): 1655-1663. (in Chinese)
- Zhu, C. Q., Chen, H. Y., Meng, Q. S. and Wang, R. 2014b. Microscopic characterization of intra-pore structures of calcareous sands. *Rock and Soil Mechanics*, 2014b, 35(7): 1831-1836. (in Chinese)
- Zhu, C. Q., Zhou, B. and Liu, H. F. 2015. State-of-the-art review of developments of laboratory tests on cemented calcareous soils. *Rock and Soil Mechanics*, 36(2): 311-319. (in Chinese)